# Schwinger boson theory of $\mathbb{Z}_2$ spin liquids

Subir Sachdev

*Department of Physics, Harvard University,*
*Cambridge, Massachusetts, 02138, USA and*
*Perimeter Institute for Theoretical Physics,*
*Waterloo, Ontario N2L 2Y5, Canada*

(Dated: March 26, 2016)

## Abstract

We use the Schwinger boson representation of quantum spins to obtain a different perspective on $\mathbb{Z}_2$ spin liquids and their possible SET structures. The Schwinger bosons themselves become the charge $Q = \pm 1/2$, $h$ particles of the spin liquid. Similar results can be obtained using Schwinger fermions, when would then realize the $Q = \pm 1/2$, $\chi$ particles of the spin liquid.

We are interested in this chapter in Hamiltonians of the form

$$\mathcal{H} = \sum_{i,j} J_{ij} \mathbf{S}_i \cdot \mathbf{S}_j \tag{1}$$

where we consider the general case of $\mathbf{S}_i$ being spin $S$ quantum spin operators on the sites, $i$, of a 2-dimensional lattice. The $J_{ij}$ are short-ranged antiferromagnetic exchange interactions. We will mainly consider here the square and triangular lattices with nearest neighbor interactions, but the methods generalize to a wide class of lattices and interaction ranges.

A careful examination of the non-magnetic 'spin-liquid' phases requires an approach which is designed explicitly to be valid in a region well separated from Néel long range order, and preserves SU(2) symmetry at all stages. It should also be designed to naturally allow for neutral $S = 1/2$ excitations. To this end, we introduce the Schwinger boson description [1], in terms of elementary $S = 1/2$ bosons. For the group $SU(2)$ the complete set of $(2S + 1)$ states on site $i$ are represented as follows

$$|S, m\rangle \equiv \frac{1}{\sqrt{(S+m)!(S-m)!}} (s^\dagger_{i\uparrow})^{S+m} (s^\dagger_{i\downarrow})^{S-m} |0\rangle, \tag{2}$$

where $m = -S, \ldots S$ is the $z$ component of the spin ($2m$ is an integer). We have introduced two flavors of Schwinger bosons on each site, created by the canonical operator $s^\dagger_{i\alpha}$, with $\alpha = \uparrow, \downarrow$, and $|0\rangle$ is the vacuum with no Schwinger bosons. The total number of Schwinger bosons, $n_s$, is the same for all the states; therefore

$$s^\dagger_{i\alpha} s^\alpha_i = n_s \tag{3}$$

with $n_s = 2S$ (we will henceforth assume an implied summation over repeated upper and lower indices). It is not difficult to see that the above representation of the states is completely equivalent to the following operator identity between the spin and Schwinger boson operators

$$S_{ia} = \frac{1}{2} s^\dagger_{i\alpha} \, \sigma^{a\alpha}{}_\beta \, s^\beta_i \tag{4}$$

where $a = x, y, z$ and the $\sigma^a$ are the usual $2 \times 2$ Pauli matrices.

Note that the Schwinger bosons, $s_\alpha$ are (roughly) the 'square root' of the Holstein-Primakoff bosons, $b$, considered in the previous chapter. In particular, for $S = 1/2$, $S_+ = s^\dagger_\uparrow s_\downarrow \sim b$. So the Schwinger boson $s_\uparrow$ ($s_\downarrow$) carries Holstein-Primakoff boson number $Q = -1/2$ ($Q = 1/2$).

The spin-states on two sites $i, j$ can combine to form a singlet in a unique manner - the wavefunction of the singlet state is particularly simple in the boson formulation:

$$\left( \varepsilon^{\alpha\beta} s^\dagger_{i\alpha} s^\dagger_{j\beta} \right)^{2S} |0\rangle \tag{5}$$

Finally we note that, using the constraint (3), the following Fierz-type identity can be established

$$\left( \varepsilon^{\alpha\beta} s^\dagger_{i\alpha} s^\dagger_{j\beta} \right) \left( \varepsilon_{\gamma\delta} s^\gamma_i s^\delta_j \right) = -2\mathbf{S}_i \cdot \mathbf{S}_j + n_s^2/2 + \delta_{ij} n_s \tag{6}$$

where $\varepsilon$ is the totally antisymmetric $2 \times 2$ tensor

$$\varepsilon = \begin{pmatrix} 0 & 1 \\ -1 & 0 \end{pmatrix} \tag{7}$$

This implies that $\mathcal{H}$ can be rewritten in the form (apart from an additive constant)

$$\mathcal{H} = -\frac{1}{2} \sum_{<ij>} J_{ij} \left( \varepsilon^{\alpha\beta} s^\dagger_{i\alpha} s^\dagger_{j\beta} \right) \left( \varepsilon_{\gamma\delta} s^\gamma_i s^\delta_j \right) \tag{8}$$

This form makes it clear that $\mathcal{H}$ counts the number of singlet bonds.

We have so far defined a one-parameter ($n_s$) family of models $\mathcal{H}$ for a fixed realization of the $J_{ij}$. Increasing $n_s$ makes the system more classical and a large $n_s$ expansion is therefore not suitable for studying the quantum-disordered phase. For this reason we introduce a second parameter - the flavor index $\alpha$ on the bosons is allowed to run from $1 \ldots 2N$ with $N$ an arbitrary integer. This therefore allows the bosons to transform under $SU(2N)$ rotations. However the $SU(2N)$ symmetry turns out to be too large. We want to impose the additional restriction that the spins on a pair of sites be able to combine to form a singlet state, thus generalizing the valence-bond structure of $SU(2)$ - this valence-bond formation is clearly a crucial feature determining the structure of the quantum disordered phase. It is well-known that this is impossible for $SU(2N)$ for $N > 1$ - there is no generalization of the second-rank, antisymmetric, invariant tensor $\varepsilon$ to general $SU(2N)$.

The proper generalization turns out to be to the group $Sp(N)$ [2]. This group is defined by the set of $2N \times 2N$ unitary matrices $U$ such that

$$U^T \mathcal{J} U = \mathcal{J} \tag{9}$$

where

$$\mathcal{J}_{\alpha\beta} = \mathcal{J}^{\alpha\beta} = \begin{pmatrix} & 1 & & & \\ -1 & & & & \\ & & & 1 & \\ & & -1 & & \\ & & & & \ddots \\ & & & & & \ddots \end{pmatrix} \tag{10}$$

is the generalization of the $\varepsilon$ tensor to $N > 1$. It is clear that $Sp(N) \subset SU(2N)$ for $N > 1$, while $Sp(1) \cong SU(2)$. The $s^\alpha_i$ bosons transform as the fundamental representation of $Sp(N)$; the "spins" on the lattice therefore belong to the symmetric product of $n_s$ fundamentals, which is also an irreducible representation. Valence bonds

$$\mathcal{J}^{\alpha\beta} s^\dagger_{i\alpha} s^\dagger_{j\alpha} \tag{11}$$

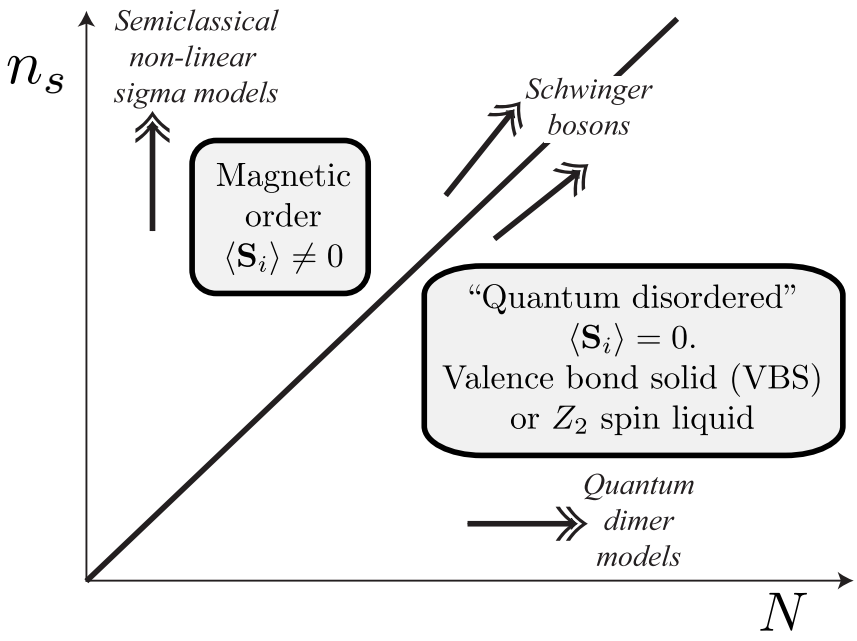


FIG. 1. Phase diagram of the 2D $Sp(N)$ antiferromagnet $\mathcal{H}$ as a function of the "spin" $n_s$. The "quantum disordered" region preserves Sp($N$) spin rotation invariance, and there is no magnetic long-range order; however, the ground states here have new types of emergent order (VBS or $Z_2$ topological order), which are described in the text.

can be formed between any two sites; this operator is a singlet under $Sp(N)$ because of (9). The form (8) of $\mathcal{H}$ has a natural generalization to general $Sp(N)$:

$$\mathcal{H} = -\sum_{i>j} \frac{J_{ij}}{2N} \left( \mathcal{J}^{\alpha\beta} s^\dagger_{i\alpha} s^\dagger_{j,\beta} \right) \left( \mathcal{J}_{\gamma\delta} s^\gamma_i s^\delta_j \right) \tag{12}$$

where the indices $\alpha, \beta, \gamma, \delta$ now run over $1 \ldots 2N$. We recall also that the constraint (3) must be imposed on every site of the lattice.

We now have a two-parameter $(n_s, N)$ family of models $\mathcal{H}$ for a fixed realization of the $J_{ij}$. It is very instructive to consider the phase diagram of $\mathcal{H}$ as a function of these two parameters (Fig. 1).

The limit of large $n_s$, with $N$ fixed leads to the semi-classical theory. For the special case of $SU(2)$ antiferromagnets with a two-sublattice collinear Néel ground state, the semiclassical fluctuations are described by the $O(3)$ non-linear sigma model. For other models, the structure of the non-linear sigma models is rather more complicated and will not be considered here.

A second limit in which the problem simplifies is $N$ large at fixed $n_s$ [3, 4], which is taken using the Schwinger fermion representation. It can be shown that in this limit the ground state is "quantum disordered". Further, the low-energy dynamics of $\mathcal{H}$ is described by an effective quantum-dimer model [4, 5], with each dimer configuration representing a particular pairing of the

sites into valence-bonds. There have been extensive studies of such quantum dimer models which we will not review here. All the quantum dimer model studies in the "quantum disordered" region of Fig. 1 have yielded phases which were obtained earlier [2] by the methods to be described below.

The most interesting solvable limit is obtained by fixing the ratio of $n_s$ and $N$

$$\kappa = \frac{n_s}{N} \tag{13}$$

and subsequently taking the limit of large $N$. The implementation of $\mathcal{H}$ in terms of bosonic operators also turns out to be naturally suited for studying this limit. The parameter $\kappa$ is arbitrary; tuning $\kappa$ modifies the slope of the line in Fig. 1 along which the large $N$ limit is taken. From the previous limits discussed above, one might expect that the ground state of $\mathcal{H}$ has magnetic long range order (LRO) for large $\kappa$ and is quantum-disordered for small $\kappa$. We will indeed find below that for any set of $J_{ij}$ there is a critical value of $\kappa = \kappa_c$ which separates the magnetically ordered and the quantum disordered phase.

## I. MEAN-FIELD THEORY

We begin by analyzing $\mathcal{H}$ at $N = \infty$ with $n_s = \kappa N$. As noted above, this limit is most conveniently taken using the bosonic operators. We may represent the partition function of $\mathcal{H}$ by

$$Z = \int \mathcal{D}\mathcal{Q}\mathcal{D}b\mathcal{D}\lambda \exp\left(-\int_0^\beta \mathcal{L} d\tau\right), \tag{14}$$

where

$$\mathcal{L} = \sum_i \left[ s_{i\alpha}^\dagger \left(\frac{d}{d\tau} + i\lambda_i\right) s_i^\alpha - i\lambda_i n_s \right] + \sum_{<i,j>} \left[ N\frac{J_{ij}|\mathcal{Q}_{i,j}|^2}{2} - \frac{J_{ij}\mathcal{Q}_{i,j}^*}{2}\mathcal{J}_{\alpha\beta} s_i^\alpha s_j^\beta + H.c. \right]. \tag{15}$$

Here the $\lambda_i$ fix the boson number of $n_s$ at each site; $\tau$-dependence of all fields is implicit; $\mathcal{Q}$ was introduced by a Hubbard-Stratonovich decoupling of $\mathcal{H}$. An important feature of the lagrangian $\mathcal{L}$ is its $U(1)$ gauge invariance under which

$$\begin{aligned} s_{i\alpha}^\dagger &\to s_{i\alpha}^\dagger(i) \exp\left(i\rho_i(\tau)\right) \\ \mathcal{Q}_{i,j} &\to \mathcal{Q}_{i,j} \exp\left(-i\rho_i(\tau) - i\rho_j(\tau)\right) \\ \lambda_i &\to \lambda_i + \frac{\partial \rho_i}{\partial \tau}(\tau). \end{aligned} \tag{16}$$

The functional integral over $\mathcal{L}$ faithfully represents the partition function, but does require gauge fixing.

The $1/N$ expansion of the free energy can be obtained by integrating out of $\mathcal{L}$ the $2N$-component $b$,$\bar{b}$ fields to leave an effective action for $\mathcal{Q}$, $\lambda$ having co-efficient $N$ (because $n_s \propto N$). Thus the

$N \to \infty$ limit is given by minimizing the effective action with respect to "mean-field" values of $\mathcal{Q} = \bar{\mathcal{Q}}$, $i\lambda = \bar{\lambda}$ (we are ignoring here the possibility of magnetic LRO which requires an additional condensate $x^\alpha = \langle b^\alpha \rangle$). This is in turn equivalent to solving the mean-field Hamiltonian

$$\mathcal{H}_{MF} = \sum_{<i,j>} \left( N \frac{J_{ij} |\bar{\mathcal{Q}}_{ij}|^2}{2} - \frac{J_{ij} \bar{\mathcal{Q}}^*_{i,j}}{2} \mathcal{J}_{\alpha\beta} s_i^\alpha s_j^\beta + H.c. \right) + \sum_i \bar{\lambda}_i (s^\dagger_{i\alpha} s_i^\alpha - n_s) \tag{17}$$

This Hamiltonian is quadratic in the boson operators and all its eigenvalues can be determined by a Bogoluibov transformation. This leads in general to an expression of the form

$$\mathcal{H}_{MF} = E_{MF}[\bar{\mathcal{Q}}, \bar{\lambda}] + \sum_\mu \omega_\mu [\bar{\mathcal{Q}}, \bar{\lambda}] \gamma^\dagger_{\mu\alpha} \gamma^\alpha_\mu \tag{18}$$

The index $\mu$ extends over $1 \ldots$.number of sites in the system, $E_{MF}$ is the ground state energy and is a functional of $\bar{\mathcal{Q}}$, $\bar{\lambda}$, $\omega_\mu$ is the eigenspectrum of excitation energies which is also a function of $\bar{\mathcal{Q}}$, $\bar{\lambda}$, and the $\gamma^\alpha_\mu$ represent the bosonic eigenoperators. The excitation spectrum thus consists of non-interacting spinor bosons. The ground state is determined by minimizing $E_{MF}$ with respect to the $\bar{\mathcal{Q}}_{ij}$ subject to the constraints

$$\frac{\partial E_{MF}}{\partial \bar{\lambda}_i} = 0 \tag{19}$$

The saddle-point value of the $\bar{\mathcal{Q}}$ satisfies

$$\bar{\mathcal{Q}}_{ij} = \langle \mathcal{J}_{\alpha\beta} s_i^\alpha s_j^\beta \rangle \tag{20}$$

Note that $\bar{\mathcal{Q}}_{ij} = -\bar{\mathcal{Q}}_{ji}$ indicating that $\bar{\mathcal{Q}}_{ij}$ is a directed field - an orientation has to be chosen on every link.

These saddle-point equations have been solved for the square and triangular lattices with nearest neighbor exchange $J$, and they lead to stable and translationally invariant solutions for $\bar{\lambda}_i$ and $\bar{\mathcal{Q}}_{ij}$. The only saddle-point quantity which does not have the full symmetry of the lattice is the orientation of the $\bar{\mathcal{Q}}_{ij}$. Note that although it appears that the choice of orientation appears to break inversion or reflection symmetries, such symmetries are actually preserved: the $\bar{\mathcal{Q}}_{ij}$ are not gauge-invariant, and all gauge-invariant observables do preserve all symmetries of the underlying Hamiltonian. For the square lattice, we have $\bar{\lambda}_i = \bar{\lambda}$, $\bar{\mathcal{Q}}_{i,i+\hat{x}} = \bar{\mathcal{Q}}_{i,i+\hat{y}} = \bar{\mathcal{Q}}$. Similarly, on the triangular lattice we have $\bar{\mathcal{Q}}_{i,i+\hat{e}_p} = \bar{\mathcal{Q}}$ for $p = 1, 2, 3$, where the unit vectors

$$\begin{aligned} \hat{e}_1 &= (1/2, \sqrt{3}/2) \\ \hat{e}_2 &= (1/2, -\sqrt{3}/2) \\ \hat{e}_3 &= (-1, 0) \end{aligned} \tag{21}$$

point between nearest neighbor sites of the triangular lattice. We sketch the orientation of the $\bar{\mathcal{Q}}_{ij}$ on the triangular lattice in Fig. 2.

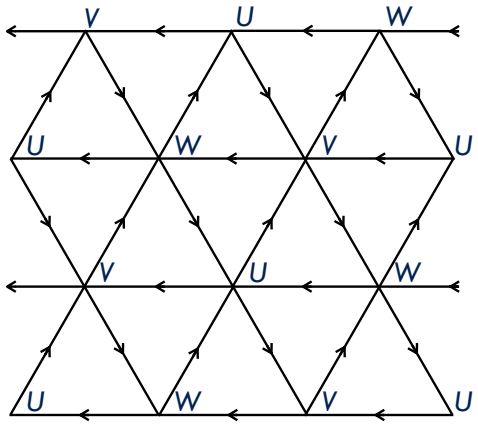


FIG. 2. Orientation of the nearest neighbor $\bar{\mathcal{Q}}_{ij}$ on the triangular lattice. Also shown are the labels of the 3 sublattices.

We can also compute the dispersion $\omega_{\boldsymbol{k}}$ of the $\gamma_{\boldsymbol{k}}$ excitations. These are bosonic particles which carry spin $S = 1/2$ ('spinons'), and so they carry fractionalized boson number charge $Q = \pm 1/2$. The dispersion on the square lattice is

$$\omega_{\boldsymbol{k}} = \left(\bar{\lambda}^2 - J^2\bar{\mathcal{Q}}^2(\sin k_x + \sin k_y)^2\right)^{1/2} \tag{22}$$

while that on the triangular lattice is [6]

$$\omega_{\boldsymbol{k}} = \left(\bar{\lambda}^2 - J^2\bar{\mathcal{Q}}^2(\sin k_1 + \sin k_2 + \sin k_3)^2\right)^{1/2} \tag{23}$$

with $k_p = \boldsymbol{k}\cdot\hat{e}_p$. These are the spinons and the spinon dispersion on the triangular lattice is plotted in Fig. 3.

Notice that the spinons have minima at two degenerate points in the Brillouin zone for both lattices. For the square lattice, the minima are at $\boldsymbol{k} = \pm(\pi/2, \pi/2)$, while for the triangular lattice they are at $\boldsymbol{k} = \pm(4\pi/3, 0)$ (and at wavevectors separated from these by reciprocal lattice vectors). So there are a total of 4 spinon excitations in both cases: 2 associated with the spin degeneracy of $S_z = Q = \pm 1/2$, and 2 associated with the degeneracy in the Brillouin zone spectrum. These extra degeneracies, beyond those required by the basic topological theory of the $\mathbb{Z}_2$ spin liquid, identifies the present state as a "symmetry enriched topological" phase—a SET [7].

## II. EXCITATION SPECTRUM

We have already described the 4-fold degenerate low energy spinon excitations above. Here, we address the nature of the spin singlet excitations.

In the context of the large $N$ expansion, this question reduces to understanding the nature of the spectrum of the $\mathcal{Q}_{ij}$ and $\lambda_i$ fluctuations about the large $N$ saddle point described above. At

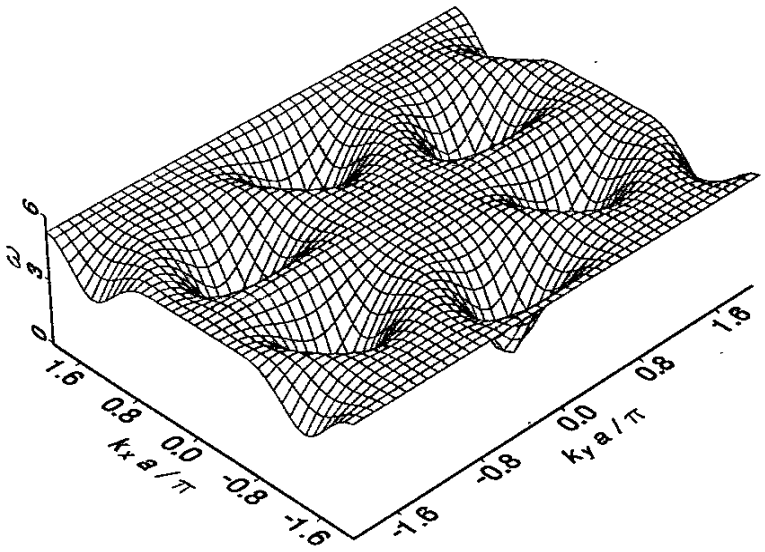


FIG. 3. Spinon dispersion on the triangular lattice.

the outset, we can view such fluctuations as composites of 2-spinon excitations, as both $\mathcal{Q}_{ij}$ and $\lambda_i$ couple to spinon pair operators, and so conclude that such excitations should not be viewed as the 'elementary' excitations of the quantum state found so far. Furthermore, the saddle-point has not broken any global symmetries of the Hamiltonian, and so it would appear that no such composite excitations has any reason to be low energy without fine-tuning.

However, it does turn out that there are separate elementary excitations in the singlet sector, and these arise from two distinct causes: $(i)$ the gauge invariance in (16) leads to a gapless "photon" excitation; $(ii)$ there are topologically non-trivial configurations of $\mathcal{Q}_{ij}$ which lead to excitations which would be not be evident in a naive $1/N$ expansion. Excitations in the class $(i)$ arise in the square lattice case, while those in class $(ii)$ appear on the triangular lattice, and these will be considered separately in the following subsections.

### A. Gauge excitations

The gauge transformations in (16) act on the phases of the $\mathcal{Q}_{ij}$, and so it is appropriate to just focus on the fluctuations of the phases of the $\mathcal{Q}_{ij}$ which are non-zero in the large $N$ limit. We will separate the discussions for the square and triangular lattices, because the results are very different.

### 1. *Square lattice*

We define

$$\begin{aligned}\mathcal{Q}_{i,i+\hat{x}} &= \bar{\mathcal{Q}} \exp\left(i\Theta_{ix}\right) \\ \mathcal{Q}_{i,i+\hat{y}} &= \bar{\mathcal{Q}} \exp\left(i\Theta_{iy}\right)\end{aligned} \tag{24}$$

Then, the gauge transformations in (16) can be written as

$$\begin{aligned}\Theta_{ix}(\tau) &\to \Theta_{ix}(\tau) - \rho_i(\tau) - \rho_{i+x}(\tau) \\ \Theta_{iy}(\tau) &\to \Theta_{iy}(\tau) - \rho_i(\tau) - \rho_{i+y}(\tau) \\ \lambda_i &\to \lambda_i + \frac{\partial \rho_i}{\partial \tau}(\tau).\end{aligned} \tag{25}$$

The question before us is whether (16) imposes on us the presence of a gapless photon in the low energy and long-wavelength limit. The answer is affirmative, and the needed result is obtained by parameterizing such fluctuations as follows

$$\begin{aligned}\Theta_{ix}(\tau) &= \eta_i b_x(r,\tau) \\ \Theta_{iy}(\tau) &= \eta_i b_y(r,\tau) \\ \lambda_i &= -i\bar{\lambda} - \eta_i b_\tau(r,\tau)\end{aligned} \tag{26}$$

where the $b_\mu$ are assumed to be smooth functions of spacetime parameterized by the continuum spatial co-ordinate $r$, and imaginary time $\tau$; the factor $\eta_i = \pm 1$ on the two checkerboard sublattices of the square lattice, so that $\eta_i$ has opposite signs on any pair of nearest-neighbor sites. Then, taking the continuum limit of (25) with $\rho_i(\tau) = \eta_i \rho(r,\tau)$, we deduce from (26) that

$$\begin{aligned}b_x &\to b_x - \partial_x \rho \\ b_y &\to b_y - \partial_y \rho \\ b_\tau &\to b_\tau - \partial_\tau \rho\end{aligned} \tag{27}$$

So we reach the very important conclusion that $b_\mu$ transforms just like a continuum U(1) gauge field. Indeed, we will shortly see that this $b_\mu$ plays the same role as the $b_\mu$ gauge field in our previous discussion of $\mathbb{Z}_2$ spin liquids Lecture 6.

As in traditional field-theoretic analyses, (27) imposes the requirement that the long-wavelength action of the $b_\mu$ fluctuations must have the form

$$\mathcal{S}_b = \int d^3x \frac{1}{2K'} (\epsilon_{\mu\nu\lambda} \partial_\nu b_\lambda)^2, \tag{28}$$

and this describes a gapless $b_\mu$ photon excitation, with a suitable velocity of 'light'. So, on the square lattice, the spectrum of spin-singlet states includes a linearly-dispersing photon mode. Such

a state is a U(1) spin liquid, and not a $\mathbb{Z}_2$ spin liquid. Actually, the gapless photon of this U(1) spin liquid is ultimately not stable because of monopole tunneling events: this is involves a long and interesting store we will not explore further here [8–11]. The remainder of the discussion in this chapter will be restricted to the triangular lattice where, as we will show below, the U(1) photon is gapped by the Higgs mechanism.

### 2. *Triangular lattice*

Now we have to consider 3 separate values of $\mathcal{Q}_{ij}$ per site, and so we replace (24) by

$$\mathcal{Q}_{i,i+\hat{e}_p} = \bar{\mathcal{Q}} \exp\left(i\Theta_p\right) \tag{29}$$

where $p = 1, 2, 3$, the vectors $\hat{e}_p$ were defined (21), $\bar{\mathcal{Q}}$ is the mean-field value, and $\Theta_p$ is a real phase. The effective action for the $\Theta_p$ must be invariant under

$$\Theta_p \to \Theta_p - \rho_i - \rho_{i+\hat{e}_p}. \tag{30}$$

Upon performing a Fourier transform, with the link variables $\Theta_p$ places on the center of the links, the gauge invariance takes the form

$$\Theta_p(\boldsymbol{k}) \to \Theta_p(\boldsymbol{k}) - 2\rho(\boldsymbol{k}) \cos(k_p/2) \tag{31}$$

The momentum $\boldsymbol{k}$ takes values in the first Brillouin zone of the triangular lattice. This invariance implies that the effective action for the $\Theta_p$ can only be a function of the following gauge-invariant combinations:

$$I_{pq} = 2\cos(k_q/2)\Theta_p(\boldsymbol{k}) - 2\cos(k_p/2)\Theta_q(\boldsymbol{k}) \tag{32}$$

We now wish to take the continuum limit at points in the Brillouin zone where the action involves only gradients of the $\Theta_p$ fields and thus has the possibility of gapless excitations. The same analysis could have been applied to the square lattice, in which case there is only one invariant $I_{xy}$. In this case, we choose $\boldsymbol{k} = \boldsymbol{g} + \boldsymbol{q}$, with $\boldsymbol{g} = (\pi, \pi)$ (this corresponds to the choice of $\eta_i$ above) and $\boldsymbol{q}$ small; then $I_{xy} = q_x\Theta_y - q_y\Theta_x$ which is clearly the U(1) flux invariant under (27).

The situation is more complex for the case of the triangular lattice [6]. Now there are 3 independent $I_{pq}$ invariants, and it is not difficult to see that only two of the three values of $\cos(k_p/2)$ can vanish at any point of the Brillouin zone. One such point is the wavevector

$$\boldsymbol{g} = \frac{2\pi}{\sqrt{3}a}(0, 1) \tag{33}$$

where

$$\begin{aligned} \boldsymbol{g} \cdot \hat{e}_1 &= \pi \\ \boldsymbol{g} \cdot \hat{e}_2 &= -\pi \\ \boldsymbol{g} \cdot \hat{e}_3 &= 0. \end{aligned} \tag{34}$$

Taking the continuum limit with the fields varying with momenta with close to $\boldsymbol{g}$ we find that the $I_{pq}$ depend only upon gradients of $\Theta_1$ and $\Theta_2$. It is also helpful to parametrize the $\Theta_p$ in the following suggestive manner (analogous to (26))

$$\begin{aligned}\Theta_1(\mathbf{r}) &= ib_1(\mathbf{r})e^{i\boldsymbol{g}\cdot\mathbf{r}} \\ \Theta_2(\mathbf{r}) &= -ib_2(\mathbf{r})e^{i\boldsymbol{g}\cdot\mathbf{r}} \\ \Theta_3(\mathbf{r}) &= H(\mathbf{r})e^{i\boldsymbol{g}\cdot\mathbf{r}}\end{aligned} \tag{35}$$

It can be verified that the condition for the reality of $\Theta_p$ is equivalent to demanding that $b_1, b_2, H$ be real. We will now take the continuum limit with $b_1, b_2, H$ varying slowly on the scale of the lattice spacing. It is then not difficult to show that the invariants $I_{pq}$ then reduce to (after a Fourier transformation):

$$\begin{aligned}I_{12} &= \partial_2 b_1 - \partial_1 b_2 \\ I_{31} &= \partial_1 H - 2b_1 \\ I_{32} &= \partial_2 H - 2b_2,\end{aligned} \tag{36}$$

where $\partial_i$ is the spatial gradient along the direction $\hat{e}_i$. Thus the $b_1, b_2$ are the components of a U(1) gauge field, with the components are taken along an 'oblique' co-ordinate system defined by the axes $\hat{e}_1, \hat{e}_2$; this is just as in the square lattice. However, in addition to $I_{12}$, we also have the invariants $I_{31}$ and $I_{32}$ in the triangular lattice; we observe that this involves the field $H$ which transforms like the phase of charge $\pm 2$ Higgs field under the U(1) gauge invariance. So the fluctuations will be characterized by an action of the form

$$\mathcal{S}_b = \int d^3x \frac{1}{2K'} \left[ I_{12}^2 + I_{31}^2 + I_{32}^2 \right], \tag{37}$$

which replaces (28). This is the action expected in the *Higgs phase* of a U(1) gauge theory. The Higgs condensate gaps out the U(1) photon, and so there are no gapless singlet excitations on the triangular lattice. This is a necessary condition for mapping the present state onto a $\mathbb{Z}_2$ spin liquid.

The presentation so far of the gauge fluctuations described by a charge $\pm 2$ Higgs field coupled to a U(1) gauge field would be appropriate for an anisotropic triangular lattice in which the couplings along the $\hat{e}_3$ direction are different from those along $\hat{e}_1$ and $\hat{e}_2$. For an isotropic triangular lattice, all three directions must be treated equivalently, and then there is no simple way to take the continuum limit in the gauge sector: we have to work with the action in (37), but with the invariants specified as in (32). Such an action does not have a gapless photon anywhere in the Brillouin zone, and all gauge excitations remain gapped. There are other choices for the wavevector $\boldsymbol{g}$ in (33) at which the other pairs of values of $\cos(k_p/2)$ vanish; these are the points

$$\frac{2\pi}{\sqrt{3}} \left( \frac{\sqrt{3}}{2}, -\frac{1}{2} \right) \quad , \quad \frac{2\pi}{\sqrt{3}} \left( \frac{-\sqrt{3}}{2}, -\frac{1}{2} \right), \tag{38}$$

which are related to the analysis above by the rotational symmetry of the triangular lattice.

### B. Topological excitations

The analysis in Section II A described small fluctuations in the phases of the $\mathcal{Q}_{ij}$ about their saddle-point values $\bar{\mathcal{Q}}$. On the triangular lattice, we found that such fluctuations led only to gapped excitations, which could even become part of the two-spinon continuum.

Now we consider excitations which involve large deviations from the spatially uniform saddle point values, and which turn out to be topologically protected. To obtain such solutions we look for spatially non-uniform solutions of the saddle-point equations (19) and (20). In general, solving such equations is a demanding numerical task, and so we will be satisfied with a simplified analysis which is valid when the spin gap is large. In the large spin gap limit, we can integrate out the Schwinger bosons, and write the energy as a local functional of the $\mathcal{Q}_{ij}$. This functional is strongly constrained by the gauge transformations in (16): for time-independent $\mathcal{Q}_{ij}$, this functional takes the form

$$E[\{\mathcal{Q}_{ij}\}] = -\sum_{i<j}\left(\alpha|\mathcal{Q}_{ij}|^2 + \frac{\beta}{2}|\mathcal{Q}_{ij}|^4\right) - K\prod_{\text{even loops}}\mathcal{Q}_{ij}\mathcal{Q}^*_{jk}\ldots\mathcal{Q}^*_{\ell i} \tag{39}$$

Here $\alpha$, $\beta$, and $K$ are coupling constants determined by the parameters in the Hamiltonian of the antiferromagnet. We have shown them to be site-independent, because we have only displayed terms in which all links/loops are equivalent; they can depend upon links/loops for longer range couplings provided the full lattice symmetry is preserved.

We can now search for saddle points of the energy functional in (39). However, from the structure of the vison states described in Lecture 6, we can anticipate that there may be saddle points $\mathcal{Q}^v_{ij}$ with the following structure. Far from the center of the vison, we have $|\mathcal{Q}^v_{ij}| = \bar{\mathcal{Q}}$, so that the energy differs from the ground state energy only by a finite amount. Closer to the center there are differences in the magnitudes. However, the key difference is in the signs of the link variables, as illustrated in Fig. 4: there is a 'branch-cut' emerging from the vison core along which $\text{sgn}(\mathcal{Q}^v_{ij}) = -\text{sgn}(\bar{\mathcal{Q}}_{ij})$. The results of a numerical minimization [12] of $E[\{\mathcal{Q}_{ij}\}]$ on the the triangular lattice are shown in Fig. 4. The magnitudes of $\mathcal{Q}^v_{ij}$ are suppressed close to the vison, and converge to $\bar{\mathcal{Q}}_{ij}$ as we move away from the vison (modulo the sign change associated with the branch cut), analogous to the Abrikisov vortices. Despite the branch-cut breaking the 3-fold rotation symmetry, the gauge-invariant fluxes of $\mathcal{Q}^v_{ij}$ preserve the rotation symmetry.

So we have found a stable real-vortex solution which preserves time-reversal, and has a finite excitation energy. We have also anticipated that this vortex will be identified with the vison particle of the $\mathbb{Z}_2$ spin liquid: this has not yet been established, and we will turn to this question in the next section.

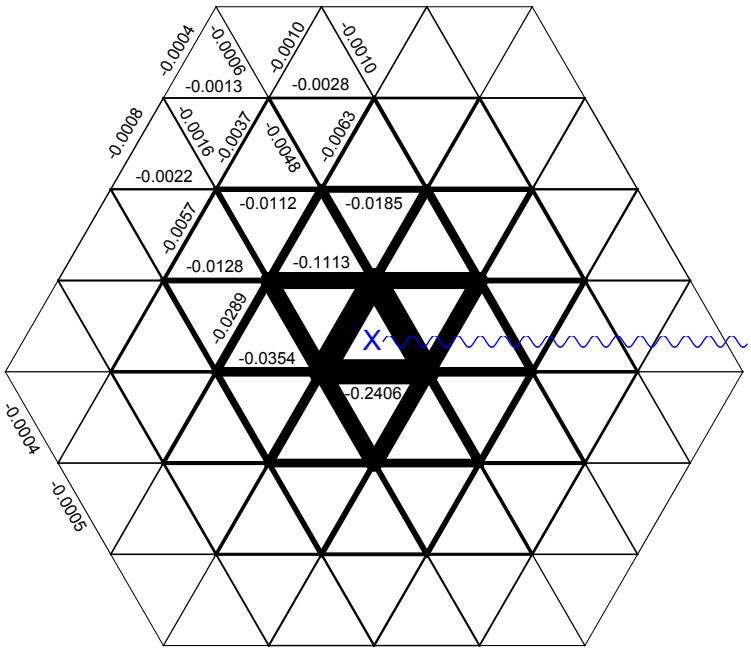


FIG. 4. A vison on the triangular lattice [12]. The center of the vison is marked by the X. The wavy line is the 'branch-cut' where we have $\mathrm{sgn}(\mathcal{Q}^v_{ij}) = -\mathrm{sgn}(\bar{\mathcal{Q}}_{ij})$ only on the links crossed by the line. Plotted is the minimization result of $E[\{\bar{\mathcal{Q}}_{ij}\}]$ with $\alpha = 1, \beta = -2, K = 0.5$. Minimization is done with the cluster embedded in a vison-free lattice with all nearest neighbor links equal to $\bar{\mathcal{Q}}_{ij}$. The numbers are $(\bar{\mathcal{Q}}_{ij} - \mathcal{Q}^v_{ij})$ and the thickness of the links are proportional to $(\mathcal{Q}^v_{ij} - \bar{\mathcal{Q}}_{ij})^{1/2}$.

## III. DYNAMICS OF EXCITATIONS

For the case of the triangular lattice, Section II has identified two types of elementary excitations: bosonic spinons with a 2-fold spin and a 2-fold lattice degeneracy, and a topological excitation which we have anticipated will become with vison particle of a $\mathbb{Z}_2$ spin liquid. We will now describe the dynamics of the interactions between these excitations, and indeed verify that they reproduce the general structure associated with the $\mathbb{Z}_2$ spin liquid.

### A. Bosonic spinons

The general structure of the theory controlling the low energy spectrum becomes clearer upon taking a suitable continuum limit of the Lagrangian in (15), while replacing $\mathcal{Q}_{ij} = \bar{\mathcal{Q}}_{ij}$ and $i\lambda_i = \bar{\lambda}$. We take the continuum limit after separating 3 sites, $U$, $V$, $V$, in each unit cell (see Fig. 2). We write the boson operators on these sites as $s^\alpha_U = U_\alpha$, $s^\alpha_V = V_\alpha$ etc. Then to the needed order in

spatial gradients, the Lagrangian density becomes [13]

$$\begin{aligned}\mathcal{L} = U_\alpha^* \frac{\partial U_\alpha}{\partial \tau} + V_\alpha^* \frac{\partial V_\alpha}{\partial \tau} + W_\alpha^* \frac{\partial W_\alpha}{\partial \tau} + \bar{\lambda}\left(|U_\alpha|^2 + |V_\alpha|^2 + |W_\alpha|^2\right) \\ - \frac{3J\bar{\mathcal{Q}}}{2}\mathcal{J}_{\alpha\beta}\left(U_\alpha V_\beta + V_\alpha W_\beta + W_\alpha U_\beta\right) + \text{c.c.} \\ + \frac{3J\bar{\mathcal{Q}}}{8}\mathcal{J}_{\alpha\beta}\left(\vec{\nabla}U_\alpha \cdot \vec{\nabla}V_\beta + \vec{\nabla}V_\alpha \cdot \vec{\nabla}W_\beta + \vec{\nabla}W_\alpha \cdot \vec{\nabla}U_\beta\right] + \text{c.c.} \end{aligned} \tag{40}$$

We now perform a unitary transformation to new variables $X_\alpha$, $Y_\alpha$, $Z_\alpha$. These are chosen to diagonalize only the non-gradient terms in $\mathcal{L}$.

$$\begin{aligned}\begin{pmatrix} U_\alpha \\ V_\alpha \\ W_\alpha \end{pmatrix} = \frac{Z_\alpha}{\sqrt{6}}\begin{pmatrix} 1 \\ \zeta \\ \zeta^2 \end{pmatrix} + \mathcal{J}_{\alpha\beta}\frac{Z_\beta^*}{\sqrt{6}}\begin{pmatrix} -i \\ -i\zeta^2 \\ -i\zeta \end{pmatrix} + \frac{Y_\alpha}{\sqrt{6}}\begin{pmatrix} 1 \\ \zeta \\ \zeta^2 \end{pmatrix} + \mathcal{J}_{\alpha\beta}\frac{Y_\beta^*}{\sqrt{6}}\begin{pmatrix} i \\ i\zeta^2 \\ i\zeta \end{pmatrix} \\ + \frac{X_\alpha}{\sqrt{3}}\begin{pmatrix} 1 \\ 1 \\ 1 \end{pmatrix}. \end{aligned} \tag{41}$$

where $\zeta \equiv e^{2\pi i/3}$. The tensor structure above makes it clear that this transformation is rotationally invariant, and that $X_\alpha$, $Y_\alpha$, $Z_\alpha$ transform as spinors under SU(2) spin rotations (for convenience, we consider the case Sp(1)≡ SU(2) in this section). Inserting Eq. (41) into $\mathcal{L}$ we find

$$\begin{aligned}\mathcal{L} = X_\alpha^* \frac{\partial X_\alpha}{\partial \tau} + Y_\alpha^* \frac{\partial Z_\alpha}{\partial \tau} + Z_\alpha^* \frac{\partial Y_\alpha}{\partial \tau} + (\bar{\lambda} - 3\sqrt{3}J\bar{\mathcal{Q}}/2)|Z_\alpha|^2 + (\bar{\lambda} + 3\sqrt{3}J\bar{\mathcal{Q}}/2)|Y_\alpha|^2 + \bar{\lambda}|X_\alpha|^2 \\ + \frac{3J\bar{\mathcal{Q}}\sqrt{3}}{8}\left(|\partial_x Z_\alpha|^2 + |\partial_y Z_\alpha|^2\right) + \ldots \end{aligned} \tag{42}$$

The ellipses indicate omitted terms involving spatial gradients in the $X_\alpha$ and $Y_\alpha$ which we will not keep track of. This is because the fields $Y_\alpha$ and $X_\alpha$ are massive relative to $Z_\alpha$, and so can be integrated out. This yields the effective Lagrangian

$$\mathcal{L}_Z = \frac{1}{(\bar{\lambda} + 3\sqrt{3}J\bar{\mathcal{Q}}/2)}|\partial_\tau Z_\alpha|^2 + \frac{3J\bar{\mathcal{Q}}\sqrt{3}}{8}\left(|\partial_x Z_\alpha|^2 + |\partial_y Z_\alpha|^2\right) + (\bar{\lambda} - 3\sqrt{3}J\bar{\mathcal{Q}}/2)|Z_\alpha|^2 + \ldots \tag{43}$$

Note that the omitted spatial gradient terms in $X_\alpha$, $Y_\alpha$ do contribute a correction to the spatial gradient term in (43), and we have not accounted for this.

So we reach the important conclusion that the spinons are described by a relativistic complex scalar field $Z_\alpha$. Counting the two values of $\alpha$, and the particle and anti-pariticle excitations, we have a total of 4 spinons, as expected.

Next, we consider the higher order terms in (43), which will arise from including the fluctuations of the gapped fields $Q$ and $\lambda$. Rather than computing these from the microscopic Lagrangian, it is more efficient to deduce their structure from symmetry considerations. The representation in (41), and the connection of the $U$, $V$, $W$ to the lattice degrees of freedom, allow us to deduce the following symmetry transformations of the $X$, $Y$, $Z$:

- Under a global spin rotation by the SU(2) matrix $g_{\alpha\beta}$, we have $Z_\alpha \to g_{\alpha\beta} Z_\beta$, and similarly for $Y$, and $Z$.

- Under a 120° lattice rotation, we have $U_\alpha \to V_\alpha$, $V_\alpha \to W_\alpha$, $W_\alpha \to U_\alpha$. From (41), we see that this symmetry is realized by

$$Z_\alpha \to \zeta Z_\alpha \ , \ Y_\alpha \to \zeta Y_\alpha \ , \ X_\alpha \to X_\alpha. \tag{44}$$

  Note that this is distinct from the SU(2) rotation because $\det(\zeta) \neq 1$.

It is easy to verify that Eq. (42) is invariant under all the symmetry operations above. These symmetry operators make it clear that the only allowed quartic term for the Heisenberg Hamiltonian is $\left(\sum_\alpha |Z_\alpha|^2\right)^2$: this quartic term added to $\mathcal{L}^Z$ yields a theory with O(4) symmetry.

We also observe from (43) that the $Z_\alpha$ field will condense when $(\bar{\lambda} - 3\sqrt{3}J\bar{\mathcal{Q}}/2)$ changes sign. This condensation breaks the spin rotation symmetry, and leads to coplanar antiferromgnetic long-range order. The $\mathbb{Z}_2$ spin liquid to coplanar antiferromagnet phase transition is therefore described by the O(4) Wilson-Fisher critical theory [14, 15].

### B. Motion of visons

Let us now consider the motion of the vison elementary excitation illustrated in Fig. 4. The vison is located at the center of a triangle, and so can tunnel between neighboring triangular cells. We are interested here in any possible Berry phases the vison could pick up upon tunneling around a closed path.

In Section II B, we characterized the vison by the saddle-point configuration $\mathcal{Q}^v_{ij}$ of the bond variables in the Hamiltonian (17). By diagonalizing this Hamiltonian [6, 12], we can show that the wavefunction of the vison can be written as

$$|\Psi^v\rangle = \mathcal{P} \exp\left(\sum_{i<j} f^v_{ij}\, \mathcal{J}_{\alpha\beta} s^\dagger_{i\alpha} s^\dagger_{j\beta}\right) |0\rangle, \tag{45}$$

where $|0\rangle$ is the boson vaccum, $\mathcal{P}$ is a projection operator which selects only states which obey (3), and the boson pair wavefunction $f^v_{ij} = -f^v_{ji}$ is determined from (17) by a Bogoliubov transformation.

Let us now consider the motion of a single vison [12]. The gauge-invariant Berry phases are those associated with a periodic motion, and so let us consider the motion of a vison along a general closed loop $\mathcal{C}$. We illustrate the simple case where $\mathcal{C}$ encloses a single site of the triangular lattice in Fig. 5. As long as the vison wavefunction can be chosen to be purely real, it is clear that no Berry phase is accumulated from the time-evolution of the wavefunction as the vison tunnels around the path $\mathcal{C}$. However, there can still be a non-zero Berry phase because a gauge-transformation is

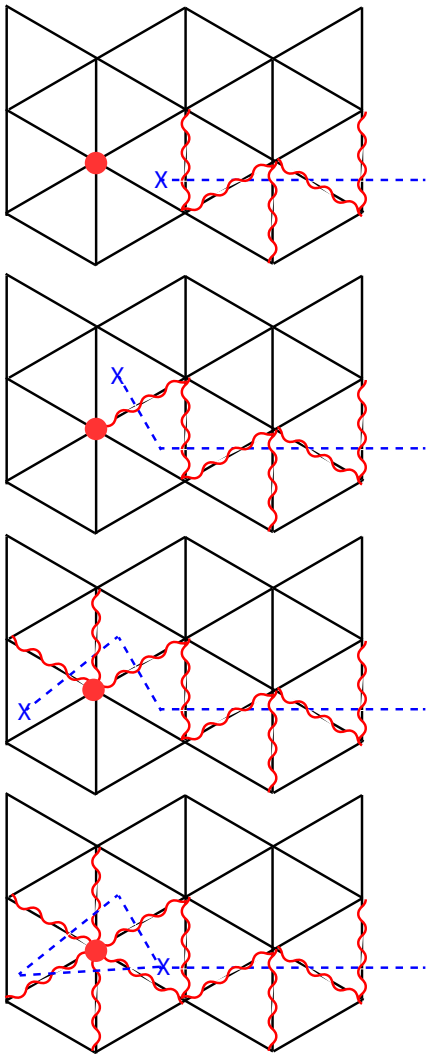

FIG. 5. Periodic motion of a vison around a closed loop $\mathcal{C}$ on the triangular lattice [12]. Here $\mathcal{C}$ encloses the single site marked by the filled circle. The wavy lines indicate $\text{sgn}(\mathcal{Q}^v_{ij}) = -\text{sgn}(\bar{\mathcal{Q}}_{ij})$, as in Fig. 4. The bottom state is gauge-equivalent to the top state, after the gauge transformation $s^\alpha_i \to -s^\alpha_i$ only for the site $i$ marked by the filled circle.

required to map the final state to the initial state. The analysis in Fig. 5 shows that the required gauge transformation is

$$\begin{aligned} s^\alpha_i &\to -s^\alpha_i, \quad \text{for } i \text{ inside } \mathcal{C} \\ s^\alpha_i &\to s^\alpha_i, \quad \text{for } i \text{ outside } \mathcal{C}. \end{aligned} \tag{46}$$

By Eq. (3), each site has $n_s$ bosons, and so the total Berry phase accumulated by $|\Psi^v\rangle$ is

$$\pi n_s \times (\text{number of sites enclosed by } \mathcal{C})\,. \tag{47}$$

So far the important case of $S = 1/2$, the vison experiences a flux of $\pi$ for every site of the triangular lattice.

It should now be clear that this $\pi$-flux is precisely that discussed in Lecture 6 for the case of bosons at half filling: there we found that the single-vortices (which eventually turned into visons in the insulating phases) also experienced a $\pi$-flux for each lattice site. And via the Holstein-Primakoff transformation, the half-filled boson case does indeed correspond to antiferromagnets with spin $S = 1/2$.

The consequences of this $\pi$-flux are similar to those in Lecture 5: it induces degeneracies in the vison spectrum, and the visons transform projectively under space group operations. Note that these are SET features of the vison sector of the $\mathbb{Z}_2$ spin liquid, not part of the basic topological structure.

### C. Mutual semions

Finally, to complete the identification of the present Schwinger boson spin liquid with the $\mathbb{Z}_2$ spin liquid, we need to establish that the spinons and visons are mutual semions. This is immediately apparent from a glance at Fig. 4. The $\mathcal{Q}^v_{ij}$ transport the visons from site to site, and for spinon encircling a vison in a large circuit, the only difference between the cases with and without the vison is the branch cut. This branch cut yields an additional phase of $\pi$ in the vison amplitude, and provides the needed phase for mutual semion statistics [2, 16].

More formally, for the case of an anisotropic triangular lattice [17], we can also write down a Chern-Simons field theory which describes both the spinon and vison sectors in a single action. We combine the gauge field analysis in Section II A 2 with the spinon continuum limit in Section III A to obtain an action [18] for the spinons $Z_\alpha$, the charge 2 Higgs field $\mathcal{H} \sim e^{iH}$, and the gauge field $b_\mu$. In the action written here, we ignore spatial anisotropies and velocities, and use a relativistic short-hand to illustrate the basic ingredients:

$$\mathcal{S}_{Z\mathcal{H}} = \int d^3x \Big[ |(\partial_\mu - ib_\mu) Z_\alpha|^2 + r_z |Z_\alpha|^2 + u_z \left(|Z_\alpha|^2\right)^2 + |(\partial_\mu - 2ib_\mu)\mathcal{H}|^2 + r_h |\mathcal{H}|^2 + u_h \left(|\mathcal{H}|^2\right)^2 - \lambda\, \mathcal{H}^* \left(\mathcal{J}^{\alpha\beta} Z_\alpha \partial_3 Z_\beta\right) + \text{c.c.} + \ldots \Big]. \quad (48)$$

The Higgs field, $\mathcal{H}$, must be condensed, $\langle \mathcal{H} \rangle = \mathcal{H}_0 \neq 0$ (and the $Z_\alpha$ spinons gapped) to obtain the $\mathbb{Z}_2$ spin liquid: only in this case does the gauge field sector reduce to (37). This action should appear familiar from our earlier discussion of vortices and double vortices in Lecture 6: it has a deceptively similar structure, but is a dual description in the boson sector. Now the tri-linear term coupling between the spinons and the Higgs field is required by spin rotation symmetry to have spatial gradient: this leads to incommensurate spin fluctuations in the presence of the Higgs condensate [18].

To transform (48) into the canonical form needed for a $\mathbb{Z}_2$ spin liquid, we need to apply the particle-to-vortex duality to the Higgs field $\mathcal{H}$: its dual will be the complex vison field $V$, which is coupled to a new gauge field $a_\mu$. The complex nature of $V$ reflects the double degeneracy of the visons, induced by the $\pi$-flux discussed in Section III B. The action for the spinons $Z_\alpha$, and the visons $V$, is then

$$\mathcal{S}_{ZV} = \int d^3x \Big[ |(\partial_\mu - ib_\mu) Z_\alpha|^2 + r_z |Z_\alpha|^2 + u_z \left(|Z_\alpha|^2\right)^2 - \lambda \, \mathcal{H}_0^* \left(\mathcal{J}^{\alpha\beta} Z_\alpha \partial_3 Z_\beta\right) + \text{c.c.} \\ + |(\partial_\mu - ia_\mu) V|^2 + r_v |V|^2 + u_v \left(|V|^2\right)^2 + \frac{i}{\pi} \epsilon_{\mu\nu\lambda} b_\mu \partial_\nu a_\lambda \ldots \Big]. \tag{49}$$

Now both $Z_\alpha$ and $V$ are gapped in the $\mathbb{Z}_2$ spin liquid, and the action has the canonical form of a topological field theory with a Chern-Simons term with $K$ matrix

$$K = \begin{pmatrix} 0 & 2 \\ 2 & 0 \end{pmatrix}. \tag{50}$$

The additional symmetry-related structure in the action for the spinons, $Z_\alpha$, and visons, $V$ describes the SET framework. The full phase diagram of (49), including negative values of $r_z$ and $r_v$, is explored in Ref. 17.


[1] D. P. Arovas and A. Auerbach, "Functional integral theories of low-dimensional quantum Heisenberg models," Phys. Rev. B **38**, 316 (1988).

[2] N. Read and S. Sachdev, "Large $N$ expansion for frustrated quantum antiferromagnets," Phys. Rev. Lett. **66**, 1773 (1991).

[3] I. Affleck and J. B. Marston, "Large-$n$ limit of the Heisenberg-Hubbard model: Implications for high-$T_c$ superconductors," Phys. Rev. B **37**, 3774 (1988).

[4] N. Read and S. Sachdev, "Some features of the phase diagram of the square lattice SU($N$) antiferromagnet," Nucl. Phys. B **316**, 609 (1989).

[5] D. S. Rokhsar and S. A. Kivelson, "Superconductivity and the quantum hard-core dimer gas," Phys. Rev. Lett. **61**, 2376 (1988).

[6] S. Sachdev, "Kagome and triangular-lattice Heisenberg antiferromagnets: Ordering from quantum fluctuations and quantum-disordered ground states with unconfined bosonic spinons," Phys. Rev. B **45**, 12377 (1992).

[7] X. Chen, Z.-C. Gu, Z.-X. Liu, and X.-G. Wen, "Symmetry protected topological orders and the group cohomology of their symmetry group," Phys. Rev. B **87**, 155114 (2013), arXiv:1106.4772 [cond-mat.str-el].

[8] N. Read and S. Sachdev, "Valence-bond and spin-Peierls ground states of low-dimensional quantum antiferromagnets," Phys. Rev. Lett. **62**, 1694 (1989).

[9] N. Read and S. Sachdev, "Spin-Peierls, valence-bond solid, and Néel ground states of low-dimensional quantum antiferromagnets," Phys. Rev. B **42**, 4568 (1990).

[10] T. Senthil, A. Vishwanath, L. Balents, S. Sachdev, and M. P. A. Fisher, "Deconfined Quantum Critical Points," Science **303**, 1490 (2004), cond-mat/0311326.

[11] T. Senthil, L. Balents, S. Sachdev, A. Vishwanath, and M. P. A. Fisher, "Quantum criticality beyond the Landau-Ginzburg-Wilson paradigm," Phys. Rev. B **70**, 144407 (2004), cond-mat/0312617.

[12] Y. Huh, M. Punk, and S. Sachdev, "Vison states and confinement transitions of $\mathbb{Z}_2$ spin liquids on the kagome lattice," Phys. Rev. B **84**, 094419 (2011), arXiv:1106.3330 [cond-mat.str-el].

[13] Y. Huh, L. Fritz, and S. Sachdev, "Quantum criticality of the kagome antiferromagnet with Dzyaloshinskii-Moriya interactions," Phys. Rev. B **81**, 144432 (2010), arXiv:1003.0891 [cond-mat.str-el].

[14] A. V. Chubukov, T. Senthil, and S. Sachdev, "Universal magnetic properties of frustrated quantum antiferromagnets in two dimensions," Phys. Rev. Lett. **72**, 2089 (1994), cond-mat/9311045.

[15] A. V. Chubukov, S. Sachdev, and T. Senthil, "Quantum phase transitions in frustrated quantum antiferromagnets," Nucl. Phys. B **426**, 601 (1994), cond-mat/9402006.

[16] X. G. Wen, "Mean-field theory of spin-liquid states with finite energy gap and topological orders," Phys. Rev. B **44**, 2664 (1991).

[17] C. Xu and S. Sachdev, "Global phase diagrams of frustrated quantum antiferromagnets in two dimensions: Doubled Chern-Simons theory," Phys. Rev. B **79**, 064405 (2009), arXiv:0811.1220 [cond-mat.str-el].

[18] S. Sachdev and N. Read, "Large $N$ Expansion for Frustrated and Doped Quantum Antiferromagnets," Int. J. Mod. Phys. B **5**, 219 (1991), cond-mat/0402109.